


RESEARCH ARTICLE

WILEY

Proteomic analysis revealed modulations of carbon and nitrogen by arbuscular mycorrhizal fungi associated with the halophyte *Suaeda salsa* in a moderately saline environment

Fengwei Diao^{1,2} | Bingbing Jia¹ | Xiuhong Wang² | Junqing Luo¹ |
Yazhou Hou¹ | Frank Yonghong Li¹ | Wei Guo¹ 

¹Inner Mongolia Key Laboratory of Environmental Pollution Control and Waste Resource Recycle, Ministry of Education Collaborative Innovation Center for Grassland Ecological Security, Ministry of Education Key Laboratory of Ecology and Resource Use of the Mongolian Plateau, School of Ecology and Environment, Inner Mongolia University, Hohhot, PR China

²State Key Laboratory of Integrative Sustainable Dryland Agriculture (in preparation), Shanxi Institute of Organic Dryland Farming, Shanxi Agricultural University, Taiyuan, PR China

Correspondence

Wei Guo, Inner Mongolia Key Laboratory of Environmental Pollution Control and Waste Resource Recycle, Ministry of Education Collaborative Innovation Center for Grassland Ecological Security, Ministry of Education Key Laboratory of Ecology and Resource Use of the M, Inner Mongolia University, 235 West University Road, Hohhot 010021, Inner Mongolia, PR China.
Email: ndguowei@163.com

Funding information

Major Science and Technology Projects in Inner Mongolia Autonomous Region, Grant/Award Numbers: 2020ZD0020, ZDZX2018054; National Natural Science Foundation of China, Grant/Award Numbers: 31860170, 41977113; Natural Science Foundation of Inner Mongolia, Grant/Award Number: 2018MS04003

Abstract

Halophytes can grow well in moderately salty habitats that restrain most plant growth. Arbuscular mycorrhizal fungi (AMF) can assist its host plants to effectively mitigate salinity stress. However, less information is available on the molecular mechanisms of AMF related to halophytes in adapting to moderate saline environments. A pot experiment was undertaken to detect the effects of AMF on the carbon (C), nitrogen (N) and phosphorus (P) concentrations in the halophyte *Suaeda salsa* which was grown at 100 mM NaCl and the underlying proteomic modulating mechanisms. The results proved that AMF decreased the N and P concentrations, increased the C, N and P accumulations and the C:N and C:P ratios. Proteomic analysis screened 581 differentially abundant proteins (DAP), which were mostly categorized in carbohydrate metabolism, energy metabolism and folding, sorting and degradation pathways. The enrichment analysis illuminated that the DAPs were assembled in 'carbon fixation in photosynthetic organisms,' 'nitrogen metabolism' and 'N-glycan biosynthesis' pathways, which might be associated with the stoichiometric changes. The integrative proteomic and transcriptomic analysis detected 64 DAP whose regulations were concordant with those of the corresponding differentially expressed genes. Furthermore, these proteins were enriched in 'carbon fixation in photosynthetic organisms' and some amino acid metabolism pathways. The modulations of these pathways might be correlated with C and N allocations and plant growth in moderate saline conditions. The study supplements the comprehension of the roles of AMF in halophytes grown in saline ecosystems.

KEYWORDS

arbuscular mycorrhizal fungi, halophyte, proteomic, saline soil, resource allocation

1 | INTRODUCTION

Global climate change and increasing anthropogenic activities have aggravated soil salinization, with the areas of saline soil increasing in recent decades (Flowers & Muscolo, 2015; Shao et al., 2019). More than one-third of the arable land in the world is currently subjected to

soil and land degradation due to salt stress (Shao et al., 2019). Soil salinity has negative effects on the growth and reproduction of the majority of plants, thereby reducing crop yield and farm productivity (Bedre et al., 2016; Xu et al., 2020). Halophytes, which make up around 1% of the world flora and can grow to reproduce in salty settings of 200 mM NaCl or more (Flowers & Colmer, 2008). Previous

research on halophytes have shed light on the physiological and molecular processes that allow plants to tolerate salt stress (Flowers & Muscolo, 2015). However, the mechanisms of halophytes in association with microorganisms to accommodate salt environments have been hardly elaborated. Understanding the mechanisms is beneficial to develop their potential values in agriculture and other ecosystem services.

Arbuscular mycorrhizal fungi (AMF) play significant roles in ecological functioning activities, such as nutrients uptake and transfer, plant growth stimulation, and plant interactions with other biota (Powell & Rillig, 2018; Tedersoo et al., 2020), particularly boosting plant tolerance to stress (Porter et al., 2020). AMF can regulate the physiology of halophytes and thereby alleviate serious salt stress (Hajiboland et al., 2015; Zhang et al., 2014). For instance, the AMF *Glomus mosseae* can promote plant biomass and the growth of the halophyte *S. salsa* at 400 mM NaCl by elevating leaf superoxide dismutase and leaf catalase activity (Li et al., 2012). However, little is known about the molecular mechanisms of AMF affecting the growth and production of halophytes in moderate saline environments. Some halophytes can show optimal growth (Flowers & Colmer, 2008), and higher root colonization can always be observed on arbuscular mycorrhizal (AM) symbiosis in moderate salinity (Diao, Dang, Xu, et al., 2021; Hajiboland et al., 2015). The influences of AMF on plant growth and production differ between moderate and high saline conditions (Diao, Dang, Xu, et al., 2021), and a tremendously positive effect may occur at moderate saline conditions.

Soil salinity usually may lead to the imbalance of ion homeostasis, metabolic confusion, the proliferation of reactive oxygen species (ROS) in plants, which may further result in osmotic stress and toxicity stress and inhibit plant development (Acosta-Motos et al., 2017; Zelm et al., 2020). Furthermore, plant response and adjustment to the salt environment are always accompanied by energy depletion and carbon translocation (Shabala et al., 2020). Plants modify osmolytes and antioxidants in response to salt stress, resulting in a drop in growth rate because a result of the reallocation of energy sources to the synthesis of organic solutes and enzymes (Munns & Gilliam, 2015). This major allocation of resources is deemed impossible in plants under non-salt conditions, because it costs too many photosynthetic products, reducing their availability for plant growth. Moreover, the procedures of Na⁺ compartmentalization into the vacuole and excretion into the rhizosphere also consume energies and resources (Theerawitaya et al., 2020; Wang, Liu, et al., 2020). Previous reports have also illuminated that AMF always promotes the uptake and accumulation of nutrients to relieve salt stress (Hidri et al., 2019; Wang, Zhai, et al., 2020). Moreover, AMF can enhance plant photosynthesis and biomass production under salt stress (Kaschuk et al., 2009; Kong et al., 2019). However, some halophytes can grow better under moderate salt conditions than under non-salt conditions, such as *S. salsa* (Flowers & Colmer, 2008; Qiu et al., 2007). Due to the nature of halophytes in salt environments, AM symbiosis may trigger distinctive molecular mechanisms in halophytes to distribute nutrients and adapt to salt environments.

Omics technologies, including transcriptomics and proteomics, have been rapidly developed and widely used to identify differential

expressions and elucidate potential molecular processes (Gu et al., 2021; Song et al., 2019). Recently, proteomics technologies have been employed to identify the proteins induced by AMF, and reveal the mechanisms of AM symbiosis tolerating abiotic stresses at the protein level (Bai et al., 2019; Wu et al., 2019). For instance, the AMF *Rhizophagus intraradices* can significantly improve protein synthesis, nitrogen metabolism and ROS scavenging to boost osmotic substance biosynthesis and response to alkaline stress in a salt-alkali grass *Puccinellia tenuiflora* by proteomics (Wang et al., 2019). Jia et al. (2019) revealed that the AMF *Rhizophagus irregularis* improved Ca²⁺ signal transduction, the secondary metabolism level of phenylpropane metabolism and ROS scavenging abilities and boosted protein biosynthesis in *Elaeagnus angustifolia* seedlings under saline stress by proteomics. Therefore, it is feasible to elaborate the regulation mechanisms of AMF in halophytes in a moderate saline environment by tandem mass tag-based (TMT) quantitative proteomics analysis.

S. salsa is widely distributed in Asia, and grows in littoral and inland salt soils in China, and the species is a leaf-succulent halophytic herb that is able to accumulate salts in shoots and can be used to restore salty soils (Song & Wang, 2015). Its favorable salt concentration is from 100 to 300 mM NaCl for vigorous growth (Qiu et al., 2007). Our previous study has shown that the AMF *Funneliformis mosseae* can significantly increase the shoot dry weight by 238.5%, the shoot height by 48.3% and the shoot Na⁺ accumulation by 137.3% in *S. salsa* grown with 100 mM NaCl (Diao, Dang, Cui, et al., 2021). Also, our early transcriptomic analysis by identifying differentially expressed genes (DEG) revealed the regulation mechanisms of AMF in promoting plant growth, that is, by enriching primary metabolism, including carbohydrate and energy metabolism, and most DEG related to photosynthesis showed a down-regulation (Diao, Dang, Cui, et al., 2021). Therefore, we used TMT quantitative proteomics technology to determine the protein changes in plant shoots to corroborate the distinctive mechanisms of AMF in *S. salsa* at moderate saline environments in the present study. We monitored shoot carbon (C), nitrogen (N) and phosphorus (P) concentrations and accumulations, and shoot C:N:P ratios, and investigated protein changes in shoots of *S. salsa*. Moreover, a correlation analysis was applied between proteomic and transcriptomic data, and the DAP whose regulations were concordant with those of the corresponding DEG were filtered and analyzed. We aimed to elucidate the distinctive molecular modulations induced by AMF in *S. salsa* under a moderate saline environment, and the possible roles of AM symbiosis in the rehabilitation of salt-polluted grounds.

2 | MATERIALS AND METHODS

2.1 | Experimental design

From April 10th through August 23 2019, we conducted a pot experiment in a greenhouse at the Inner Mongolia University in Hohhot, China. The greenhouse's temperature ranged from 15 to 35°C, with a humidity level of 50%–80%. *S. salsa* was utilized as the model plant,

and inoculation of AMF (*F. mosseae*) to the plant was used as the treatment and a non-inoculated plant was used as the control. The *S. salsa* seed grew for 90 days to allow for symbiotic establishment (Li et al., 2012), and then all pots were irrigated with NaCl solutions for 45 days to maintain a salty environment until the culture finished. Each pot had six seedlings, and each treatment was replicated three times.

2.2 | Experimental materials and preparation

The bank of Glomales from the Beijing Academy of Agriculture and Forestry Sciences, China, provided the *F. mosseae* inoculum (number: BGC NM04A). The *S. salsa* seeds were obtained in China's Yellow River Delta (36°12'N, 118°50'E), and a specialist in the field of Plant Taxonomy has confirmed the seed based on the phenotype of plant and seed.

For surface sterilization, the seeds were immersed in 10% NaClO for 10 min, and then washed several times with deionized, sterile water. The plastic pot was filled into 2.5 kg autoclaved mixture (sand: soil = 1:1 mass ratio), and the form of the tub was 15 × 18 × 15 cm (lower diameter × upper diameter × height). These sands were washed three times with deionized water after first being rinsed with tapwater. The soil properties were pH 7.83, 1.38% organic matter, 10.6 mg kg⁻¹ available nitrogen, 26.4 mg kg⁻¹ available phosphorus and 55.9 mg kg⁻¹ available potassium. The soil and sand were autoclaved for 2 hr at 121°C and 0.24 MPa pressure (Wang, Zhai, et al., 2020). The inoculated groups were added with 50 g of the inoculant (a mixture of soil substrate, mycorrhizal root fragments, spores and mycelia of *F. mosseae*). The non-inoculated groups received 50 g sterilized inoculant in the same way and 30 ml filtrate (filtered inoculant using a 0.25 m filter membrane to keep the same microbial biota but devoid of mycorrhizal propagules). The seeds were sown and grew for 90 days to allow symbiotic establishment (Li et al., 2012), after which they were irrigated with NaCl solutions. A 50 mM NaCl concentration was utilized first, and then 100 mM NaCl concentration was used from the next day to the last. A threefold volume of substrate capacity was employed to keep the same salt concentration every day (Diao, Dang, Cui, et al., 2021). Hoagland solution was used to water each pot every 2 weeks. After 45 days of salt irrigation, all plants were harvested.

2.3 | Determinations of C, N and P concentrations and accumulations in plant shoots

At 70°C, the collected shoots were dried until they reached a consistent weight. The concentrations of C and N in shoot samples were determined by an elemental analyzer (CHNOS Elemental Analyzer, Elementar Co., Germany). Sulphanilamide standard reference material (S15.00-0062, Elementar Co., Germany) was used for quality control.

A total of 500 mg shoot samples were combined with 5 ml HNO₃, and digested for 96 hr at 120°C using the AIM600 digesting

apparatus. The concentrations of P in the digested solutions were determined by ICP-OES (Optima 7000 DV, PerkinElmer, USA).

The C, N and P concentrations were multiplied by the shoot dry-weight, respectively, to compute C, N and P accumulations.

2.4 | Proteomics analysis

2.4.1 | Protein extraction, digestion and TMT labeling

Based on the difference in plant growth phenotype and transcriptomics between mycorrhizal and non-mycorrhizal *S. salsa*, plant shoot samples were taken for proteome analysis (Diao, Dang, Cui, et al., 2021). On the day of harvest, the top and fresh shoots were picked and quickly frozen in liquid nitrogen before being stored at -80°C.

The shoots were ground and suspended in a 1:3 mixture of 1% PVPP and BPP buffer. The samples were centrifuged, then vortex at 4°C for 10 min with an equal volume of Tris-saturated phenol. They were centrifuged after that, and an equivalent volume of BPP buffer was added to the phenol phase, which was vortexed at 4°C for 10 min. The protein supernatants were combined with 5-fold volumes of 0.1 M ammonium acetate in methanol and stored at -20°C for 12 hr to precipitate protein. The samples were washed twice with 90% acetone after centrifugation. Finally, the dried samples were sonicated for 2 min in protein lysis buffer (1% SDS, 8 M urea) with protease inhibitor. The protein supernatant was centrifuged, and BCA Protein Assay Kit (Thermo Scientific, MA, USA) was applied to determine the quantity and concentration of the protein.

The digesting procedure was then carried out. A 100 µg protein was resuspended in TEAB buffer (triethylammonium bicarbonate) to a final concentration of 100 mM. The samples were alkylated with IAM for 40 min in the gloominess at 24°C, and then precipitated in acetone for 4 hr at -20°C. After centrifugation, the samples were incubated at 37°C overnight with trypsin (trypsin: protein = 1:50 mass ratio). Ten-plex TMT reagents were used to tag the peptides. The samples were combined and dried under a vacuum.

2.4.2 | High pH RPLC separation and LC-MS/MS analysis

To increase proteome depth, all samples were fractionated by Vanquish Flex binary UHPLC chromatography (Thermo Scientific, MA, USA) with ACQUITY UPLC BEH C18 Column (1.7 µm, 2.1 mm × 150 mm, Waters, USA). Peptides were separated first using a gradient of elution over 48 min at 200 µl per minute. The gradient elution was performed with 0%, 5%, 10%, 30%, 36% and 42%. Each sample generated 20 fractions, which were merged.

Labeled peptides were analyzed by EASY-nLC system and mass spectrometer with an ion source. The peptides were first eluted for 120 min using a C18-reversed-phase column with solvent A and

solvent B at 300 nl per minute. Solvent A contained 2% ACN and 0.1% formic acid, while the solvent B included 80% ACN and 0.1% formic acid. The Q Exactive HF-X instrument was set in DDA mode.

2.4.3 | Protein identification and quantification

PROTEOME DISCOVERER 2.4 software was used to match the RAW data files to the transcriptome of *S. salsa* (Diao, Dang, Cui, et al., 2021). The search criterion was applied at 20 ppm mass tolerance for MS and 0.02 Da for MS/MS, and the enzyme chosen as trypsin allowed two missed cleavage, and the dynamic modifications chose as methionine oxidation. Protein identifications set high confidence peptides using a 1% FDR threshold, and only the proteins with at least one unique peptide were identified. Differentially abundant proteins (DAP) were screened by R software using Student's *t*-test, and the criteria were set as $p < 0.05$ and fold change > 1.2 or < 0.83 (Gu et al., 2021; Wang et al., 2019).

2.4.4 | Bioinformatics analysis

These DAP were annotated and classified using KEGG and GO databases. The significance of protein enrichment on GO term and KEGG pathway was assessed by Fisher's exact test (p -value), and the q -value was got by rectified p -value with Benjamini and Hochberg method. Subcellular locations of the DAP were predicted using the Subloc database.

2.5 | PRM analysis

Based on the findings of the proteomic analysis, 10 DAP related to photosynthesis were selected to perform parallel reaction monitoring (PRM) quantification analysis, with the aim to confirm the credibility of TMT-based proteomic data. Protein extraction and digestion followed the same steps as the TMT test. A mass spectrometer coupled with Easy-nLC 1200 was used in the experiment. Each peptide sample was injected, and they were split by C18-reversed-phase chromatography and a linear gradient from 2% to 80% ACN, 0.1% FA with 300 nl per minute. Finally, SKYLINE software was used to analyze PRM data.

2.6 | Statistical analysis

The significant difference in shoot C, N and P concentrations or pools, and the C:N, C:P and N:P ratios between the inoculated and non-inoculated treatments were analyzed using independent samples *t*-test in SPSS 16.0 software (SPSS Inc., IL, USA). And the choices of p -values in statistical results were dependent on the result of Levenes test for equality of variances. The significance were indicated

with $^*(p < 0.05)$ and $^{**}(p < 0.01)$. All figures were pictured with the ggplot2 package in R software.

3 | RESULTS

3.1 | C, N and P concentrations and accumulations, and C:N:P ratios

AMF significantly decreased the N concentration by 32.8% and P concentration by 42.2%, but did not alter the C concentration, in-plant shoots (Table 1). AMF significantly increased the C, N and P accumulations by 244.5%, 124.9% and 91.7%, respectively. AMF significantly increased the C:N ratio by 49.2% and the C:P ratio by 76.4%, but did not alter the N:P ratio.

3.2 | Protein identification and functional annotation

The shoots of *S. salsa* with or without AMF association were analyzed using TMT quantitative proteomic technique to investigate the molecular processes of AMF assisting plants to resist or adapt to the moderate saline conditions (100 mM NaCl). The analysis generated 663,471 spectra, and further identified 131,952 spectra. A total of 61,927 peptides were found and were assigned to 8247 proteins. Mass and coverage distributions of these proteins were shown in Figure S1.

These identified proteins were functionally annotated and classified using KEGG and GO databases. A total of 4434 (53.8%) proteins were annotated in the KEGG database and mapped in 20 pathways of five branches. The proteins were mostly classified into branches of 'carbohydrate metabolism,' 'translation' and 'folding, sorting and degradation' (Figure S2). A total of 6921 (83.9%) proteins were separated

TABLE 1 C, N and P concentrations and accumulations, and C:N:P ratios in shoots of *Suaeda salsa* at 100 mM NaCl from *Funneliformis mosseae* inoculation treatment

	NaCl + NM	NaCl + AM
C concentration (mg g ⁻¹)	334.5 ± 6.4	340.4 ± 5.7
N concentration (mg g ⁻¹)	23.82 ± 3.37	16.01 ± 0.93*
P concentration (mg g ⁻¹)	5.05 ± 0.33	2.92 ± 0.24**
C accumulation (mg pot ⁻¹)	738.3 ± 151.6	2543.3 ± 433.9**
N accumulation (mg pot ⁻¹)	52.99 ± 16.28	119.17 ± 16.62**
P accumulation (mg pot ⁻¹)	11.28 ± 3.19	21.62 ± 2.40*
C:N ratio	14.27 ± 2.40	21.29 ± 0.93**
C:P ratio	66.41 ± 5.23	117.18 ± 7.80**
N:P ratio	4.71 ± 0.59	5.51 ± 0.36

Note: NaCl, 100 mM NaCl. Data are means ± standard deviation ($n = 3$). The significant difference between NaCl + AM and NaCl + NM are indicated with $^*p < 0.05$ and $^{**}p < 0.01$. Abbreviations: AM, arbuscular mycorrhizal; NM, non-mycorrhizal.

into 53 GO terms in three categories. The term 'cellular process' was the most dominant group in biological process, and the term 'catalytic activity' was the most dominant group in molecular function (Figure S3).

3.3 | Identification and subcellular localization analysis of DAP

These identified proteins were analyzed quantitatively, and a total of 581 DAP were detected in the study. Volcano plots were drawn to exhibit the significant regulation of proteins in the experiment (Figure 1). The number of upregulated proteins was 385, more than that of downregulated proteins.

The DAP were analyzed using the Subloc database to calculate the subcellular localization of proteins (Figure 1). A total of 237 (40.8%) DAP were predicted in cytoplasmic, and 70 (12.0%) DAP were localized in the chloroplast.

3.4 | Functional categorization and enrichment analysis of DAP

To further acquaintance the adjustment induced by AMF, 202 of 581 DAP were annotated and functionally classified, using the KEGG database (Figure 2). Metabolism (63.1%) and genetic information processing (26.5%) pathways occupied the high proportion.

Furthermore, carbohydrate metabolism (15.7%), energy metabolism (10.4%) and folding, sorting and degradation (9.3%) pathways owned high proportions of the DAP.

These annotated DAP were further categorized into 92 detailed pathways in the KEGG database and they were carried out enrichment analysis using software KOBAS. The pathway 'carbon fixation in photosynthetic organisms' showed the most significant enrichment and owned the most number of DAP (13 DAP). In addition, the pathways of 'nitrogen metabolism' and 'N-glycan biosynthesis' were also enrichment. The top 10 enriched pathways were showed in Figure 3 (based on q -values), including 'photosynthesis—antenna proteins' and 'pPhotosynthesis.' To further understand the pathways adjusted by AMF, 352 of 581 DAP were annotated and they have further carried out an enrichment analysis in the GO database using software GOATOOLS. Many GO terms linked to carbohydrate metabolism, molecule glycosylation and nitrogen metabolism, including 'single-organism carbohydrate metabolic process,' 'carbohydrate phosphorylation,' 'monosaccharide metabolic process,' 'photosynthesis, dark reaction,' 'reactive nitrogen species metabolic process,' 'macromolecule glycosylation,' 'protein N-linked glycosylation.' The detailed results about enriched GO terms were shown in Table S1.

3.5 | DAP related to photosynthesis in proteomics

The DAP related to photosynthetic pathways were chosen, including the pathways 'photosynthesis—antenna proteins,' 'photosynthesis'

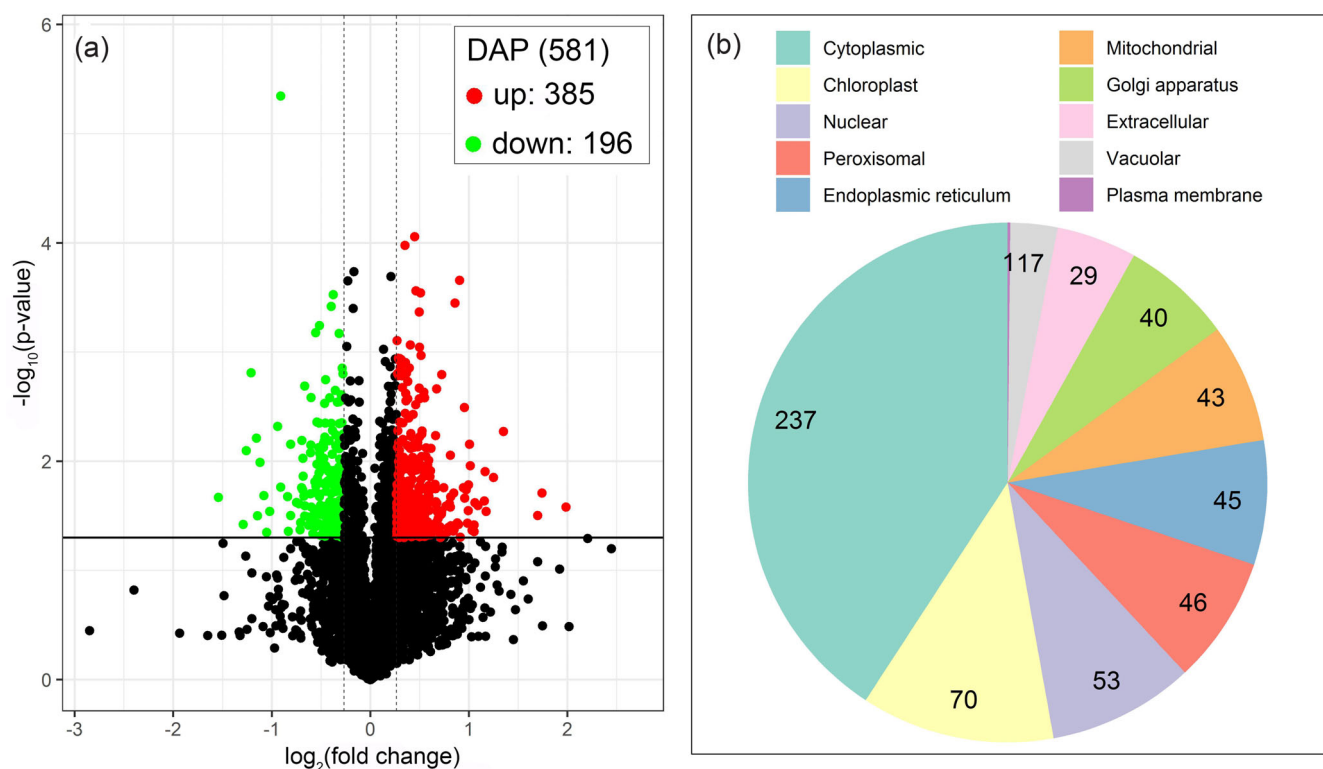


FIGURE 1 Volcano plot (a) and subcellular localization analysis (b) of DAP in shoots of *Suaeda salsa* at 100 mM NaCl from *Funneliformis mosseae* inoculation treatment [Colour figure can be viewed at [wileyonlinelibrary.com](https://onlinelibrary.wiley.com/doi/10.1002/jpl.4274)]

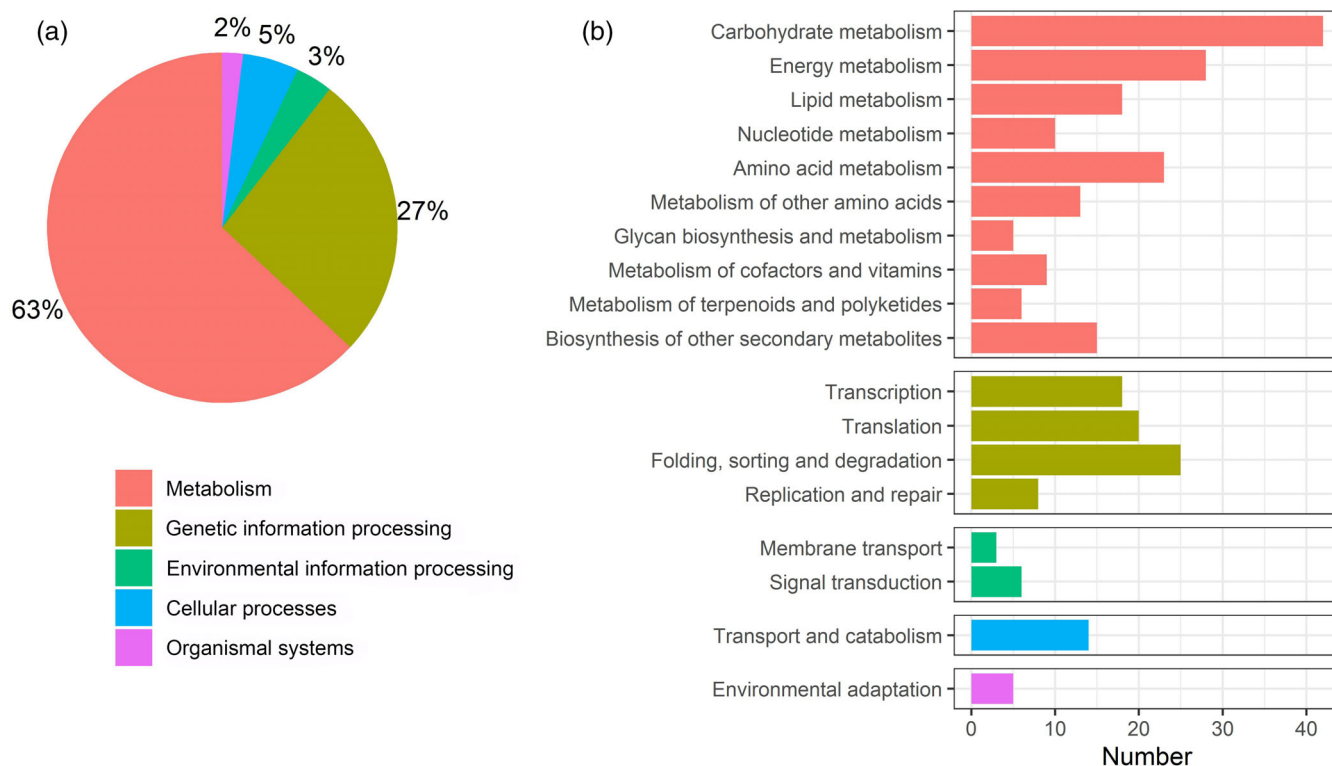


FIGURE 2 Function categorization analysis of DAP in shoots of *Suaeda salsa* at 100 mM NaCl from *Funneliformis mosseae* inoculation treatment. (a) Function categorization in level 1. (b) Function categorization in level 2 [Colour figure can be viewed at [wileyonlinelibrary.com](https://onlinelibrary.wiley.com/doi/10.1002/psp.4274)]

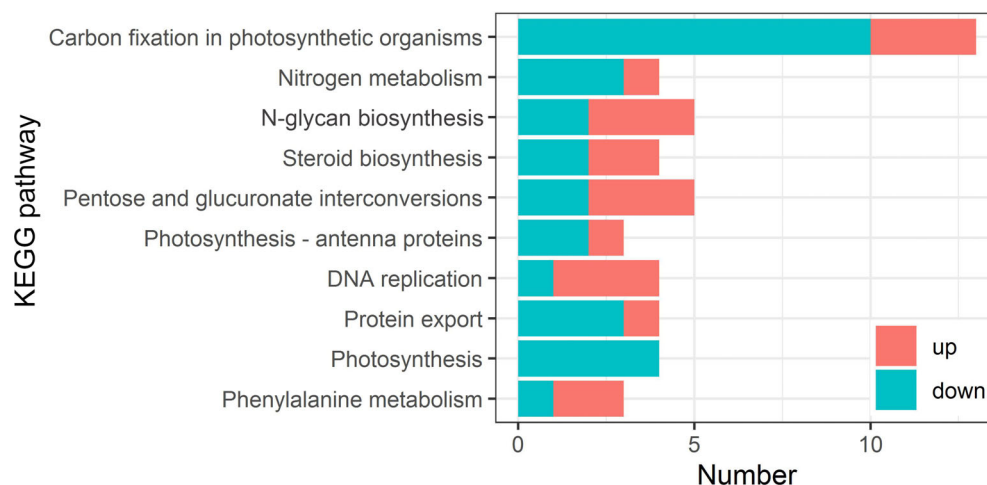


FIGURE 3 KEGG pathway enrichment analysis of DAP in shoots of *Suaeda salsa* at 100 mM NaCl from *Funneliformis mosseae* inoculation treatment. The 10 top KEGG pathways were showed in Figure 3 [Colour figure can be viewed at [wileyonlinelibrary.com](https://onlinelibrary.wiley.com/doi/10.1002/psp.4274)]

and 'carbon fixation in photosynthetic organisms' (Table 2). The abundance of proteins described as NADP-dependent malic enzymes was upregulated to the maximum level (1.40-fold) in the carbon fixation pathway. Moreover, the abundance of DAP described as ribulose biphosphate carboxylase small chain PW9 was downregulated to the maximum level (0.42-fold). In addition, the abundance of three antenna proteins were affected by AMF. Four DAP enriched in the pathway of photosynthesis showed downregulation, and the abundance of proteins described as photosystem I reaction center subunit N were decreased by 0.63-fold.

3.6 | Integrative proteomic and transcriptomic analysis

A poor Pearson correlation ($\rho = 0.0485$) was found between the protein expression ratios of proteomic and the corresponding gene expression ratios of transcriptomic (Figure S4). Interestingly, 64 DAP were identified, whose regulations were concordant with the regulations of the corresponding DEG. Moreover, the upregulated number was 18 and the downregulated number was 46. These DAP were showed in Table S2.

TABLE 2 DAP related to photosynthesis in shoots of *Suaeda salsa* at 100 mM NaCl from *Funneliformis mosseae* inoculation treatment

Accession	Description	Fold change	Regulation	p-value
Carbon fixation in photosynthetic organisms				
DN150_c0_g1_i11_orf1	NADP-dependent malic enzyme	1.40	Up	0.023
DN1282_c0_g1_i6_orf1	Phosphoglycerate kinase 3	1.37	Up	0.010
DN41_c1_g1_i5_orf1	Malate dehydrogenase	1.31	Up	0.004
DN18289_c0_g1_i1_orf1	Phosphoenolpyruvate carboxykinase (ATP)-like	0.82	Down	0.041
DN5386_c0_g2_i1_orf1	Pyruvate, phosphate dikinase	0.81	Down	0.039
DN42117_c0_g2_i1_orf1	Hypothetical protein TSUD_98560	0.79	Down	0.048
DN13790_c1_g3_i2_orf1	Aspartate aminotransferase	0.73	Down	0.048
DN5521_c0_g1_i5_orf1	Glyceraldehyde-3-phosphate dehydrogenase	0.72	Down	0.011
DN59328_c0_g1_i2_orf1	Ribulose biphosphate carboxylase small chain 3	0.71	Down	0.039
DN5468_c0_g1_i3_orf1	Glyceraldehyde-3-phosphate dehydrogenase B	0.70	Down	0.009
DN8645_c0_g1_i1_orf1	Glutamate-glyoxylate aminotransferase 2	0.70	Down	0.031
DN17707_c0_g1_i1_orf1	Glyceraldehyde-3-phosphate dehydrogenase A	0.70	Down	0.037
DN24575_c0_g1_i6_orf1	Ribulose biphosphate carboxylase small chain PW9	0.42	Down	0.008
Photosynthesis—antenna proteins				
DN36231_c0_g1_i1_orf1	Chlorophyll a-b binding protein 7	1.41	Up	0.029
DN23887_c0_g2_i1_orf1	Chlorophyll a-b binding protein 1	0.72	Down	0.016
DN6890_c0_g1_i6_orf1	Chlorophyll a-b binding protein	0.56	Down	0.044
Photosynthesis				
DN1790_c0_g2_i1_orf1	ATP synthase gamma chain	0.81	Down	0.045
DN4933_c1_g1_i1_orf1	Photosystem I reaction center subunit II	0.81	Down	0.049
DN12072_c0_g2_i1_orf1	Ferredoxin-2	0.70	Down	0.013
DN638_c0_g1_i13_orf1	Photosystem I reaction center subunit N	0.63	Down	0.032

Note: fold change, NaCl + AM vs. NaCl+NM. p-value, Student's t-test.

To further understand the function of 64 DAP, their subcellular localizations were calculated by the Subloc database, and classified functionally by the KEGG database (Figure 4). A total of 26 (40.6%) DAP were predicted in cytoplasmic and 20 (31.3%) DAP in the chloroplast. The function classification showed that 91.9% of the DAP were assigned to the metabolism pathway. Furthermore, amino acid metabolism (29.7%), energy metabolism (27.0%) and carbohydrate metabolism (18.9%) pathways owned the top three numbers. The enrichment analysis indicated that the pathway 'carbon fixation in photosynthetic organisms' had the most significant enrichment and owned six DAP. Other significantly enriched pathways (q -value <0.05) were attributed to amino acid metabolism pathway, including 'alanine, aspartate and glutamate metabolism,' 'arginine biosynthesis,' 'cysteine and methionine metabolism' and 'glycine, serine and threonine metabolism,' and all these DAP showed downregulation in mycorrhizal plants.

3.7 | PRM validation

A total of 10 DAP were selected to perform PRM analysis and confirmed the credibility of the TMT results. The validation showed that the expression tendency of these DAP in PRM analysis was highly

consistent with those in the TMT results (Figure S5). Thus, these results indicated that the proteomic analysis was highly trustworthy.

4 | DISCUSSION

Some halophytes can grow optimally under modest salt concentrations (Flowers & Colmer, 2008; Guo et al., 2018), as halophytes have evolved specific features to adapt to salt environments, such as high tolerance and regulation for Na^+ in xylem, in addition to having common salt-tolerant mechanisms they share with glycophytes (Zarei et al., 2020; Zelm et al., 2020). AMF induces different strategies in halophytes to respond to salt environments. Pan et al. (2020) expounded that AMF can lead to certain discrepancies in physiological responses to salt stress between glycophytes and halophytes. Moreover, our previous study has shown that AMF induced the DEG that are mainly enriched in carbohydrate and energy metabolism, including the pathways 'carbon fixation in photosynthetic organisms' and 'glyoxylate and dicarboxylate metabolism,' in the halophyte *S. salsa* at 100 mM NaCl, using transcriptomic analysis (Diao, Dang, Cui, et al., 2021). In this study, we further used proteomic analysis to corroborate the distinctive modulations from a view of resource allocation.

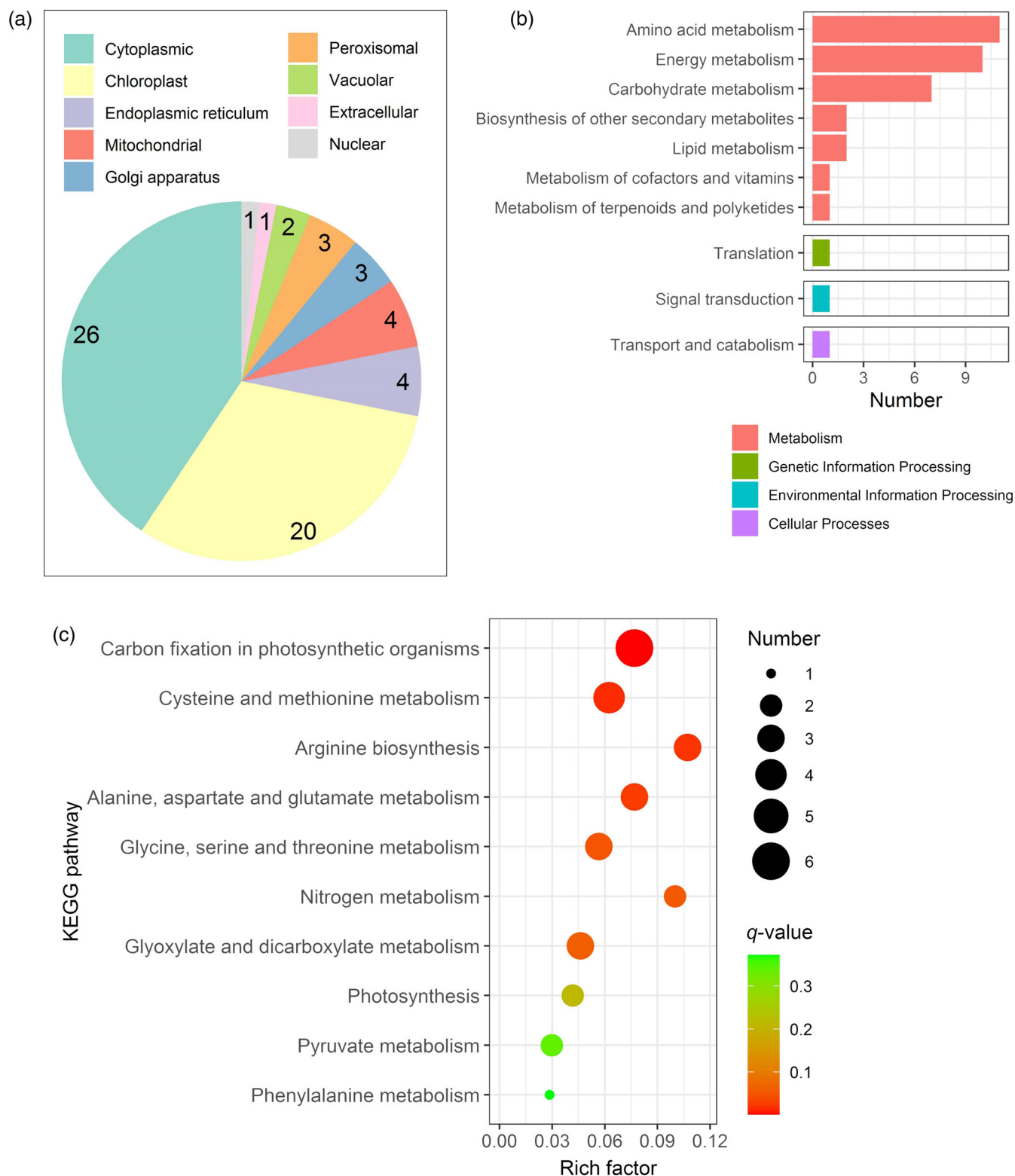


FIGURE 4 Subcellular localization analysis (a), KEGG function categorization analysis (b) and KEGG pathway enrichment analysis (c) of 64 cases of concordant regulation between DAP and DEG in proteomic and transcriptomic data [Colour figure can be viewed at [wileyonlinelibrary.com](https://onlinelibrary.wiley.com/doi/10.1002/psp.4274)]

A low correlation is detected between proteomic and transcriptomic data in our study (Figure S4), which is expected as various post-transcriptional regulatory processes equally play pivotal roles in

protein expression (Song et al., 2019). A low correlation has also been found in transcriptomic and proteomic integration analysis to explore peanut seed coat in response to pathogenic fungus infection (Zhao, Li,

et al., 2019) and photoperiod-sensitive in maize line (Song et al., 2019). However, the results of the proteomic analysis show that a total of 581 DAP (Figure 1) are mostly classified in metabolism processing, including carbohydrate metabolism, energy metabolism and amino acid metabolism (Figure 2; Table S1), which is consistent with the classification of DEG in shoots by transcriptomic analysis (Diao, Dang, Cui, et al., 2021). Wang et al. (2019) have also shown that carbohydrate metabolism, energy metabolism and amino acid metabolism are affected by AM symbiosis at 300 mM NaHCO_3 in a study of *P. tenuiflora* inoculated with AMF under tolerating alkaline stress in alkali-degraded soil. Previous studies suggest that the regulations of primary metabolism by AMF may optimize plant capacity for nutrient allocation to sustain growth (Diao, Dang, Cui, et al., 2021; Kaur & Suseela, 2020).

The variations of N and P concentrations and stoichiometry in the plant can also mirror the adjustment of nutrient allocation in cellular organs and trophic dynamics (Chen et al., 2010; Johnson, 2010). N is the essential component for all enzymes (Hidri et al., 2019), and 75% of N in plant leaf is invested in chloroplasts and thus in the procurement of C through photosynthesis (Johnson, 2010). This study shows that AMF decreases N concentration, which is in agreement with the downregulation of the abundance of most DAP related to photosynthesis, though they increase N accumulation (Tables 1 and 2). AMF did not alter C concentration, though increased C accumulation and C:N ratio (Table 1). We speculate that C assimilation can be compensated by the increase in photosynthetic areas of plants, as mycorrhizal plants have higher shoot height and other morphological features in the last phase of vegetative stages (Diao, Dang, Cui, et al., 2021). Furthermore, our enrichment analysis of the DAP indicates that the pathways of 'carbon fixation in photosynthetic organisms,' 'nitrogen metabolism' and 'N-glycan biosynthesis' are affected by AMF (Figure 3), which is correlated with the C and N modulations in plants (Table 1). These results of mycorrhizal plants having lower N concentration but higher biomass compared to non-mycorrhizal plants were also reported in clover (*Trifolium repens*) colonized by AMF (Chen et al., 2010). These suggest that AMF induce the changes in pathways related to C fixation, N metabolism and N-glycan biosynthesis, leading to the changes in N concentration and C:N ratio. Not inconsistently with our results, proteomic analysis revealed AMF induce certain DAPs related to ROS scavenging-related functions in alkali-tolerant plant *P. tenuiflora* under alkaline stress (300 mM NaHCO_3) and salt-tolerance plant *E. angustifolia* under salt stress (300 mM NaCl) (Jia et al., 2019; Wang et al., 2019). The inconsistency may imply that the regulation of AMF on these pathways in halophytes differs with the environment, that is, between under the moderate and high salinity stress. Most DAPs related to photosynthesis are downregulated (Table 2), which may trigger another possible mechanism. When the abundance of antenna proteins is downregulated, it signifies the relaxation of the harvested light, and thereby photo-inhibition can be avoided in the photosynthetic organs with salt interference (Diao, Dang, Cui, et al., 2021; Zhang et al., 2019).

The enrichment analysis of 64 DAPs concordant with DEG demonstrates that the proteins enriched in 'cysteine and methionine

metabolism,' 'arginine biosynthesis,' 'alanine, aspartate and glutamate metabolism' and 'glycine, serine and threonine metabolism' pathways, are all assigned to amino acid metabolism, and show a downregulation (Figure 4; Table S2). These regulations may be affected by the decrease of N and P concentrations (Table 1), because N is a component of amino acids and P is a component of nucleic acids, playing respectively key roles in protein and RNA synthesis (Johnson, 2010; Zhao et al., 2015). However, N and P accumulations were significantly increased, which is a consequence of the dilution effect by biomass (Chen et al., 2010), so as C:P and C:N ratios have risen in mycorrhizal plants (Table 1). These results imply that AMF has promoted C assimilation in vegetative stages that provide C resources for fast growth of plants (i.e., C accumulation) in moderate salt environments, which results in a similar shoot C concentration in inoculated and non-inoculated plants (Eroglu et al., 2020; Smith & Stitt, 2007). Moreover, three DAPs related to sugar transporter are upregulated, beneficial to carbon allocation (Zhao, Chen, et al., 2019). Therefore, AMF can readjust the balance among C assimilation, storage and growth, thus affecting N allocation in plant shoots, and attribute to the regulation of the relevant pathways, such as 'carbon fixation in photosynthetic organisms,' 'nitrogen metabolism,' 'N-glycan biosynthesis' and some amino acid metabolism pathways.

5 | CONCLUSIONS

We conclude that AMF can decrease the N concentration and increase the C:N ratio in plant shoots at 100 mM NaCl, and the alteration is associated with the regulations of 'carbon fixation in photosynthetic organisms,' 'nitrogen metabolism' and 'N-glycan biosynthesis' pathways that are enriched by the DAP in KEGG database. Moreover, AMF improves C and N accumulations. These results suggest that AMF affects the N allocation and supplies more C resources for the fast growth of halophyte *S. salsa* at the moderate saline environment. The 64 DAP concordant with DEG, identified by integrative proteomic and transcriptomic analysis, are enriched in 'carbon fixation in photosynthetic organisms' and some amino acid metabolism pathways, also indicating the possibility of resource allocation by AMF. Future researchers should pay close attention to the changes of metabolites induced by AM symbiosis and define the corresponding regulation pathways to verify the capacities for resource allocation modulated by AM symbiosis in sustained growth.

ACKNOWLEDGMENTS

This work was financially supported by the National Natural Science Foundation of China [31860170 and 41977113]; the Natural Science Foundation of Inner Mongolia [2018MS04003] and the Major Science and Technology Projects in Inner Mongolia Autonomous Region [ZDZX2018054 and 2020ZD0020].

DATA AVAILABILITY STATEMENT

Data sharing not applicable - no new data generated, or the article describes entirely theoretical research.

ORCID

Wei Guo  <https://orcid.org/0000-0003-4630-503X>

REFERENCES

- Acosta-Motos, J., Ortuño, M., Bernal-Vicente, A., Diaz-Vivancos, P., Sanchez-Blanco, M., & Hernandez, J. (2017). Plant responses to salt stress: Adaptive mechanisms. *Agronomy*, 7, 18. <https://doi.org/10.3390/agronomy7010018>
- Bai, L., Sun, H. B., Liang, R. T., & Cai, B. Y. (2019). iTRAQ proteomic analysis of continuously cropped soybean root inoculated with *Funneliformis mosseae*. *Frontiers in Microbiology*, 10, 61. <https://doi.org/10.3389/fmicb.2019.00061>
- Bedre, R., Mangu, V. R., Srivastava, S., Sanchez, L. E., & Baisakh, N. (2016). Transcriptome analysis of smooth cordgrass (*Spartina alterniflora* Loisel), a monocot halophyte, reveals candidate genes involved in its adaptation to salinity. *BMC Genomics*, 17, 657. <https://doi.org/10.1186/s12864-016-3017-3>
- Chen, M. M., Yin, H. B., O'Connor, P., Wang, Y. S., & Zhu, Y. G. (2010). C: N: P stoichiometry and specific growth rate of clover colonized by arbuscular mycorrhizal fungi. *Plant and Soil*, 326, 21–29. <https://doi.org/10.1007/s11104-009-9982-4>
- Diao, F., Dang, Z., Cui, X., Xu, J., Jia, B., Ding, S., Zhang, Z., & Guo, W. (2021). Transcriptomic analysis revealed distinctive modulations of arbuscular mycorrhizal fungi inoculation in halophyte *Suaeda salsa* under moderate salt conditions. *Environmental and Experimental Botany*, 183, 104337. <https://doi.org/10.1016/j.envexpbot.2020.104337>
- Diao, F., Dang, Z., Xu, J., Ding, S., Hao, B., Zhang, Z., Zhang, J., Wang, L., & Guo, W. (2021). Effect of arbuscular mycorrhizal symbiosis on ion homeostasis and salt tolerance-related gene expression in halophyte *Suaeda salsa* under salt treatments. *Microbiological Research*, 245, 1–10. <https://doi.org/10.1016/j.micres.2020.126688>
- Eroglu, C. G., Cabral, C., Ravnkov, S., Bak Topbjerg, H., & Wollenweber, B. (2020). Arbuscular mycorrhiza influences carbon-use efficiency and grain yield of wheat grown under pre- and post-anthesis salinity stress. *Plant Biology*, 22, 863–871. <https://doi.org/10.1111/plb.13123>
- Flowers, T. J., & Colmer, T. D. (2008). Salinity tolerance in halophytes. *The New Phytologist*, 179, 945–963. <https://doi.org/10.1111/j.1469-8137.2008.02531.x>
- Flowers, T. J., & Muscolo, A. (2015). Introduction to the special issue: Halophytes in a changing world. *AoB Plants*, 7, 1–5. <https://doi.org/10.1093/aobpla/plv020>
- Gu, N., Zhang, X., Gu, X., Zhao, L., Godana, E. A., Xu, M., & Zhang, H. (2021). Transcriptomic and proteomic analysis of the mechanisms involved in enhanced disease resistance of strawberries induced by *Rhodotorula mucilaginosa* cultured with chitosan. *Postharvest Biology and Technology*, 172, 111355. <https://doi.org/10.1016/j.postharvbio.2020.111355>
- Guo, J., Li, Y., Han, G., Song, J., & Wang, B. (2018). NaCl markedly improved the reproductive capacity of the euhalophyte *Suaeda salsa*. *Functional Plant Biology*, 45, 350–361. <https://doi.org/10.1071/FP17181>
- Hajibolani, R., Dashtebani, F., & Aliasgharzad, N. (2015). Physiological responses of halophytic C₄ grass *Aeluropus litoralis* to salinity and arbuscular mycorrhizal fungi colonization. *Photosynthetica*, 53, 572–584. <https://doi.org/10.1007/s11099-015-0131-4>
- Hidri, R., Metoui-Ben Mahmoud, O., Debez, A., Abdelli, C., Barea, J.-M., & Azcon, R. (2019). Modulation of C:N:P stoichiometry is involved in the effectiveness of a PGPR and AM fungus in increasing salt stress tolerance of *Sulla carnosus* Tunisian provenances. *Applied Soil Ecology*, 143, 161–172. <https://doi.org/10.1016/j.apsoil.2019.06.014>
- Jia, T., Wang, J., Chang, W., Fan, X., Sui, X., & Song, F. (2019). Proteomics analysis of *E. angustifolia* seedlings inoculated with arbuscular mycorrhizal fungi under salt stress. *International Journal of Molecular Sciences*, 20, 788. <https://doi.org/10.3390/ijms20030788>
- Johnson, N. C. (2010). Resource stoichiometry elucidates the structure and function of arbuscular mycorrhizas across scales. *The New Phytologist*, 185, 631–647. <https://doi.org/10.1111/j.1469-8137.2009.03110.x>
- Kaschuk, G., Kuyper, T. W., Leffelaar, P. A., Hungria, M., & Giller, K. E. (2009). Are the rates of photosynthesis stimulated by the carbon sink strength of rhizobial and arbuscular mycorrhizal symbioses? *Soil Biol. The Biochemist*, 41, 1233–1244. <https://doi.org/10.1016/j.soilbio.2009.03.005>
- Kaur, S., & Suseela, V. (2020). Unraveling arbuscular mycorrhiza-induced changes in plant primary and secondary metabolome. *Metabolites*, 10, 335. <https://doi.org/10.3390/metabo10080335>
- Kong, L., Gong, X., Zhang, X., Zhang, W., Sun, J., & Chen, B. (2019). Effects of arbuscular mycorrhizal fungi on photosynthesis, ion balance of tomato plants under saline-alkali soil condition. *Journal of Plant Nutrition*, 43, 682–698. <https://doi.org/10.1080/01904167.2019.1701029>
- Li, T., Liu, R. J., He, X. H., & Wang, B. S. (2012). Enhancement of superoxide dismutase and catalase activities and salt tolerance of euhalophyte *Suaeda salsa* L. by mycorrhizal fungus *glomus mosseae*. *Pedosphere*, 22, 217–224. [https://doi.org/10.1016/s1002-0160\(12\)60008-3](https://doi.org/10.1016/s1002-0160(12)60008-3)
- Munns, R., & Gilliam, M. (2015). Salinity tolerance of crops – What is the cost? *The New Phytologist*, 208, 668–673. <https://doi.org/10.1111/nph.13519>
- Pan, J., Peng, F., Tedeschi, A., Xue, X., Wang, T., Liao, J., Zhang, W., & Huang, C. (2020). Do halophytes and glycophytes differ in their interactions with arbuscular mycorrhizal fungi under salt stress? A meta-analysis. *Botanical Studies*, 61, 13. <https://doi.org/10.1186/s40529-020-00290-6>
- Porter, S. S., Bantay, R., Friel, C. A., Garoutte, A., Gdanetz, K., Ibarreta, K., Moore, B. M., Shetty, P., Siler, E., & Friesen, M. L. (2020). Beneficial microbes ameliorate abiotic and biotic sources of stress on plants. *Functional Ecology*, 34, 2075–2086. <https://doi.org/10.1111/1365-2435.13499>
- Powell, J. R., & Rillig, M. C. (2018). Biodiversity of arbuscular mycorrhizal fungi and ecosystem function. *The New Phytologist*, 220, 1059–1075. <https://doi.org/10.1111/nph.15119>
- Qiu, N., Chen, M., Guo, J., Bao, H., Ma, X., & Wang, B. (2007). Coordinate up-regulation of V-H⁺-ATPase and vacuolar Na⁺/H⁺ antiporter as a response to NaCl treatment in a C₃ halophyte *Suaeda salsa*. *Plant Science*, 172, 1218–1225. <https://doi.org/10.1016/j.plantsci.2007.02.013>
- Shabala, S., Chen, G., Chen, Z. H., & Pottosin, I. (2020). The energy cost of the tonoplast futile sodium leak. *The New Phytologist*, 225, 1105–1110. <https://doi.org/10.1111/nph.15758>
- Shao, H., Chu, L., Lu, H., Qi, W., Chen, X., Liu, J., Kuang, S., Tang, B., & Wong, V. (2019). Towards sustainable agriculture for the salt-affected soil. *Land Degradation & Development*, 30, 574–579. <https://doi.org/10.1002/ldr.3218>
- Smith, A. M., & Stitt, M. (2007). Coordination of carbon supply and plant growth. *Plant, Cell & Environment*, 30, 1126–1149. <https://doi.org/10.1111/j.1365-3040.2007.01708.x>
- Song, J., & Wang, B. (2015). Using euhalophytes to understand salt tolerance and to develop saline agriculture: *Suaeda salsa* as a promising model. *Annals of Botany*, 115, 541–553. <https://doi.org/10.1093/aob/mcu194>
- Song, X. H., Tian, L., Wang, S. X., Zhou, J. L., Zhang, J., Chen, Z., Wu, L.-J., Ku, L.-X., & Chen, Y.-H. (2019). Integrating transcriptomic and proteomic analyses of photoperiod-sensitive in near isogenic maize line under long-day conditions. *Journal of Integrative Agriculture*, 18, 1211–1221. [https://doi.org/10.1016/S2095-3119\(18\)62040-4](https://doi.org/10.1016/S2095-3119(18)62040-4)
- Tedersoo, L., Bahram, M., & Zobel, M. (2020). How mycorrhizal associations drive plant population and community biology. *Science*, 367, 1–9. <https://doi.org/10.1126/science.aba1223>
- Theerawitaya, C., Tisarum, R., Samphumphuang, T., Takabe, T., & Chaum, S. (2020). Expression levels of the Na⁺/K⁺ transporter OsHKT2;1

- and vacuolar Na^+/H^+ exchanger OsNHX1, Na enrichment, maintaining the photosynthetic abilities and growth performances of indica rice seedlings under salt stress. *Physiology and Molecular Biology of Plants*, 26, 513–523. <https://doi.org/10.1007/s12298-020-00769-3>
- Wang, J., Zhai, L., Ma, J., Zhang, J., Wang, G. G., Liu, X., Zhang, S., Song, J., & Wu, Y. (2020). Comparative physiological mechanisms of arbuscular mycorrhizal fungi in mitigating salt-induced adverse effects on leaves and roots of *Zelkova serrata*. *Mycorrhiza*, 30, 341–355. <https://doi.org/10.1007/s00572-020-00954-y>
- Wang, W. Y., Liu, Y. Q., Duan, H. R., Yin, X. X., Cui, Y. N., Chai, W. W., Song, X., Flowers, T. J., & Wang, S. M. (2020). SsHKT1;1 is coordinated with SsSOS1 and SsNHX1 to regulate Na^+ homeostasis in *Suaeda salsa* under saline conditions. *Plant and Soil*, 449, 117–131. <https://doi.org/10.1007/s11104-020-04463-x>
- Wang, Y., Lin, J., Huang, S., Zhang, L., Zhao, W., & Yang, C. (2019). Isobaric tags for relative and absolute quantification-based proteomic analysis of *Puccinellia tenuiflora* inoculated with arbuscular mycorrhizal fungi reveal stress response mechanisms in alkali-degraded soil. *Land Degradation & Development*, 30, 1584–1598. <https://doi.org/10.1002/ldr.3346>
- Wu, J. T., Wang, L., Zhao, L., Huang, X. C., & Ma, F. (2019). Arbuscular mycorrhizal fungi effect growth and photosynthesis of *Phragmites australis* (Cav.) Trin ex. Steudel under copper stress. *Plant Biology*, 22, 62–69. <https://doi.org/10.1111/plb.13039>
- Xu, Z., Zhou, J., Ren, T., Du, H., Liu, H., Li, Y., & Zhang, C. (2020). Salt stress decreases seedling growth and development but increases quercetin and kaempferol content in *Apocynum venetum*. *Plant Biology*, 22, 813–821. <https://doi.org/10.1111/plb.13128>
- Zarei, M., Shabala, S., Zeng, F., Chen, X., Zhang, S., Azizi, M., Rahemi, M., Davarpanah, S., Yu, M., & Shabala, L. (2020). Comparing kinetics of xylem ion loading and its regulation in halophytes and glycophytes. *Plant & Cell Physiology*, 61, 403–415. <https://doi.org/10.1093/pcp/pcz205>
- Zelm, E. V., Zhang, Y., & Testerink, C. (2020). Salt tolerance mechanisms of plants. *Annual Review of Plant Biology*, 71, 403–433. <https://doi.org/10.1146/annurev-arplant-050718-100005>
- Zhang, H. S., Qin, F. F., Qin, P., & Pan, S. M. (2014). Evidence that arbuscular mycorrhizal and phosphate-solubilizing fungi alleviate NaCl stress in the halophyte *Kosteletzkya virginica*: Nutrient uptake and ion distribution within root tissues. *Mycorrhiza*, 24, 383–395. <https://doi.org/10.1007/s00572-013-0546-3>
- Zhang, X., Han, C., Gao, H., & Cao, Y. (2019). Comparative transcriptome analysis of the garden asparagus (*Asparagus officinalis* L.) reveals the molecular mechanism for growth with arbuscular mycorrhizal fungi under salinity stress. *Plant Physiology and Biochemistry*, 141, 20–29. <https://doi.org/10.1016/j.plaphy.2019.05.013>
- Zhao, R., Guo, W., Bi, N., Guo, J., Wang, L., Zhao, J., & Zhang, J. (2015). Arbuscular mycorrhizal fungi affect the growth, nutrient uptake and water status of maize (*Zea mays* L.) grown in two types of coal mine spoils under drought stress. *Applied Soil Ecology*, 88, 41–49. <https://doi.org/10.1016/j.apsoil.2014.11.016>
- Zhao, S., Chen, A., Chen, A., Li, C., Xia, R., & Wang, X. (2019). Transcriptomic analysis reveals the possible roles of sugar metabolism and export for positive mycorrhizal growth responses in soybean. *Physiologia Plantarum*, 166, 712–728. <https://doi.org/10.1111/ppl.12847>
- Zhao, X., Li, C., Yan, C., Wang, J., Yuan, C., Zhang, H., & Shan, S. (2019). Transcriptome and proteome analyses of resistant preharvest peanut seed coat in response to *aspergillus flavus* infection. *Electronic Journal of Biotechnology*, 39, 82–90. <https://doi.org/10.1016/j.ejbt.2019.03.003>

SUPPORTING INFORMATION

Additional supporting information may be found in the online version of the article at the publisher's website.

How to cite this article: Diao, F., Jia, B., Wang, X., Luo, J., Hou, Y., Li, F. Y., & Guo, W. (2022). Proteomic analysis revealed modulations of carbon and nitrogen by arbuscular mycorrhizal fungi associated with the halophyte *Suaeda salsa* in a moderately saline environment. *Land Degradation & Development*, 33(11), 1933–1943. <https://doi.org/10.1002/ldr.4274>